

Punching Behavior of RC Flat Slabs Containing Recycled Ceramic Aggregate



Wael Ibrahim, Amal Zamrawi

Abstract: This paper examines the feasibility of replacing natural aggregate with recycled crushed ceramics in R.C flat slabs. Nowadays, many researchers are trying to use recycled ceramics as coarse aggregate in manufacturing concrete structures to decrease waste construction materials, and save raw materials. The experimental work was carried out on six slabs measuring 1650 x 1650 x 150 mm with a connected central column tested for punching shear. One slab was control without recycled ceramics aggregate; five slabs with recycled ceramics aggregate with different ratios of 20%, 35%, 50%, 60% and 70% were used.

Keywords: fire resistance, ceramics, flexural, flat slabs.

I. INTRODUCTION

Many construction and development activities today consume large amounts of concrete. The amount of construction waste is also increasing because of the demolition process. Much of this waste can be recycled to produce new products and increase the sustainability of construction projects. As recyclable construction wastes, concrete and ceramic can replace the natural aggregate in concrete because of their hard and strong physical properties. Punching failure occurs in the flat slab due to the slab having large span-to-depth ratio [1]. Ceramic waste has been classified non-biodegradable waste that is very difficult to be recycled. Environmental and economic factors increasingly encourage higher utility of industrial waste [2], recycling by a systematic investigation of the possible use of these wastes in concrete production. The compressive strength for Concrete Ceramic Waste Slab (CCWS) varied from 15MPa - 30MPa [3], CCWS has lower density compared to conventional concrete [3]. Investigation on ceramic waste and stone dust as aggregate replacement in concrete showed that the optimum percentage for replacement of stone dust with fine aggregate along with 20% replacement of coarse aggregate by ceramic waste was found to be 40% [4]. The punching resistance of RC slabs made of recycled aggregates concrete is similar to the control RC slabs and the displacement and the punching strength of the recycled aggregates concrete slabs was similar to the control RC slabs. In addition, the cracking load slightly decreases [5]. Regardless of the replacement percentage of natural coarse aggregate with recycled coarse aggregate, crack pattern under punching shear failure in all the slabs are similar. Up to 40% replacement of NCA with RCA there is a marginal

decrement in compression and split tensile strength when compared with natural coarse aggregate concrete. The experimental program was carried out using six R.C slabs with different ratios of recycled crushed ceramics to study the punching capacity, failure mode, and cracking pattern of R.C flat slabs manufactured using recycled crushed ceramics.

II. EXPERIMENTAL PROGRAM

A. Experimental program matrix

The experimental program matrix consists of six RC flat slabs. The six slabs were cast with central column; one as a control slab without adding crushed ceramics, five specimens with ratios of 20%, 35%, 50%, 60% and 70% see Fig 1. The slabs with dimension 1650 x 1650 x 150 mm with bottom reinforcement fay 10@100 mm and top reinforcement fay 10 @ 200 mm.

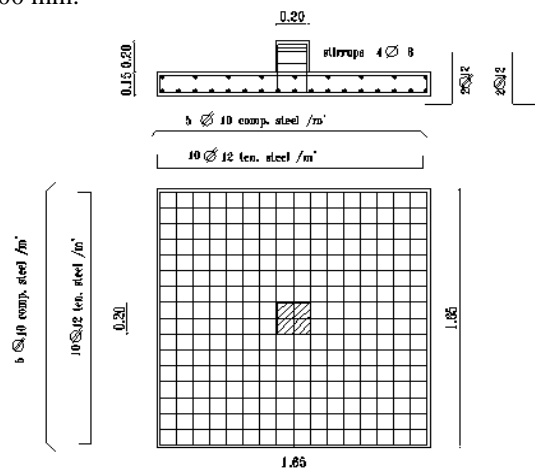


Fig. 1.Slab layout and reinforcement arrangements.

B. Material Properties

The average compressive strength of the normal / recycled concrete based on ASTM C 39 [6] is 25 MPa and the average tensile strength is 2.50 MPa. The average yield strength of steel reinforcement is 400 MPa with a modulus of elasticity of 200 GPa (DIN 50145) [7] and the ultimate strength is 600 MPa. The mix composition of the studied normal and recycled concrete is shown in Table I & II.

Table- I: Normal concrete mix composition.

Sand (kg/m ³)	450
Gravel (kg/m ³)	1100
Cement (kg/m ³)	350
Water (L/m ³)	175
W/C	0.50

Revised Manuscript Received on February 07, 2020.

* Correspondence Author

Wael Ibrahim*, Civil department, Mataria, Helwan University, Cairo, Egypt. Email: wael.Ibrahim@rwth-aachen.de

Amal Zamrawi, Civil department, Mataria, Helwan University, Cairo, Egypt. Email: amalzmrawi@gmail.com

© The Authors. Published by Blue Eyes Intelligence Engineering and Sciences Publication (BEIESP). This is an open access article under the CC BY-NC-ND license (<http://creativecommons.org/licenses/by-nc-nd/4.0/>)

Table- II: Recycled concrete mix composition.

Sand (kg/m ³)	450
recycled ceramics (kg/m ³)	1100
Cement (kg/m ³)	350
Water (kg/m ³)	175
W/C	0.50

Porous ceramic coarse aggregates" (PCCA) used in this study were obtained from ceramic industries in Egypt.

C. Test Set-up

Loading was applied at the column till failure occurs. Load versus deflection and ductility index and absorbed energy were calculated. The overall view of the test setup is shown in Fig. (1).



Fig. 2. Test Set-up for loading slabs.

III. RESULT AND DISCUSSION

From Fig.3 and Fig.4, it is clear that the load vs. displacements curves of the various concrete slabs were qualitatively similar, the punching strength of the (PCCA) slabs was similar to that of the RC slabs and the cracking load slightly decreases like. Also, as the (PCCA) increases, the load increases till 35% that get the maximum punching load see Fig.3 then. Any increase in (PCCA) more than 35% decreases the load. From Fig.4 it is clear that the minimum deflection was for the specimen contains 35% PCCA the maximum deflection was for the specimen contains 60% PCCA.

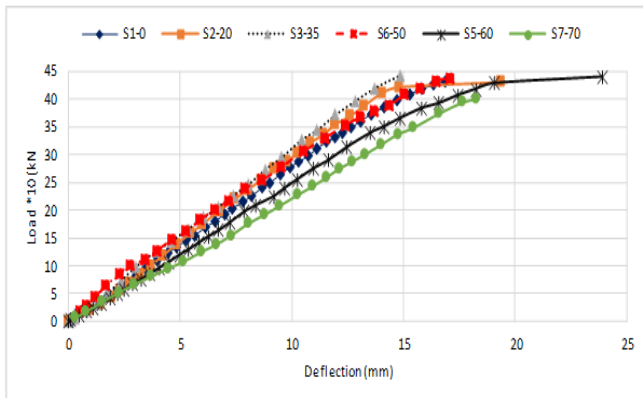


Fig. 3. Load-displacement relationship for slabs.

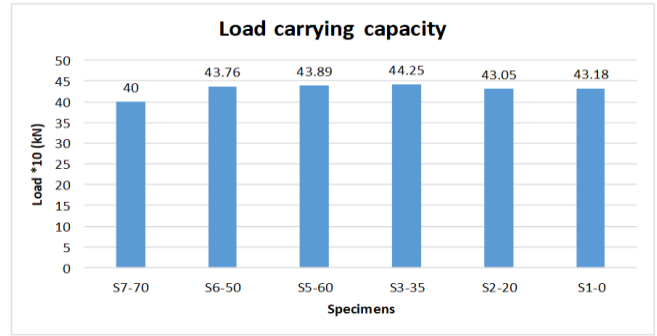


Fig. 4. Load capacity for slabs.

A. Ductility Index, Stiffness and Absorbed Energy

Ductility measures obtained from the deflection at 70% of the maximum loads. The energy absorption based on displacement was calculated as the area under the load-deflection curve for the plastic zone only. Absorbed energy is a factor that represents the amount of energy being absorbed by the slab; it's directly proportional with the ductility index, so as the ductility index increases the absorbed energy also increases see Fig.5 and Fig.6.

Initial stiffness K_i is defined as the slope of the load-deflection curve at load value less than the cracking load. The stiffness degradation ratio was calculated as the ratio between ultimate stiffness K_u and the initial stiffness K_i . The stiffness degradation ratio may be used to assess the ductility of the specimen on a way that the lower the stiffness degradation ratio, the higher is the ductility. The higher the crushed ceramic ratio was up till 35% the higher the stiffness degradation and the lower the ductility index. Table III illustrates the calculations of ductility index, Initial, ultimate stiffness, stiffness degradation and absorbed energy of all slabs.

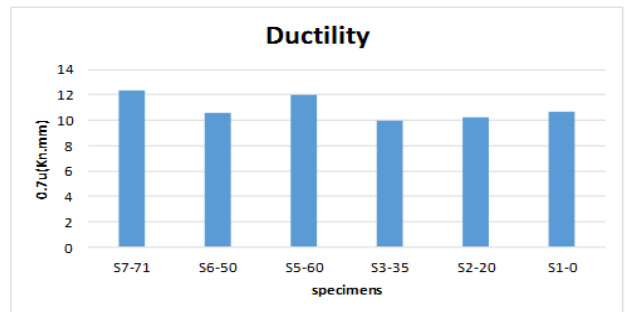


Fig. 5. Ductility index for test specimens.

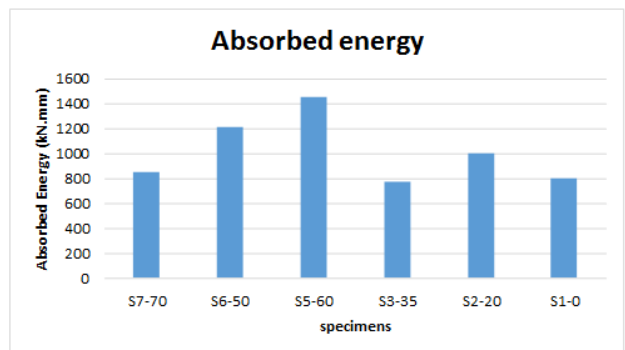


Fig. 6. Absorbed energy for test specimens.

Table- III: Calculated loads for test specimens.

ID	Cracking		Ultimate		Stiffness			Ductility index 0.7μ (mm)
	P _{cr} kN	Δ _{cr} mm	P _{ult} kN	Δ _{ult} mm	K _i = $\frac{P_{cr}}{\Delta_{cr}}$	K _u = $\frac{P_u - P_{cr}}{\Delta_u - \Delta_{cr}}$	K _u /K _i	
S1-0	141	5.28	432	16.88	26.60	25.12	0.94	10.70
S2-20	139	4.83	431	19.40	28.75	12.19	0.42	10.26
S3-35	144	4.61	443	14.86	31.20	29.12	0.93	10.00
S5-60	152	6.25	439	23.90	24.32	16.25	0.66	12.00
S6-50	162	5.40	438	17.10	29.90	23.58	0.79	10.60
S7-70	139	6.60	400	18.20	21.00	22.50	1.10	12.30

B. Code provisions

ACI code [8]

ACI 318 code for punching shear strength derived from Moe’s work on low strength concrete. The ultimate shear strength for slabs is given by Equation (1).

$$V_{uo} = u \cdot d \cdot (v_n) \tag{1}$$

Where;

(u) is the length of the critical perimeter, taken at a distance of d/2 from the column, mm.

(d) is the effective depth of slab, mm

(v_n) is the punching shear strength, MPa

British code [9]

The punching shear capacity of concrete based on British code is calculated by the by Equation (2).

$$v_c = \left(\frac{0.79}{\gamma_m} \right) \left(\frac{100A_s}{b_o \cdot d} \right)^{1/3} \left(\frac{f_{cu}}{25} \right)^{1/3} \left(\frac{400}{d} \right)^{1/4} \tag{2}$$

Where;

γ_m is safety factor =1.25

A_s is effective main steel area of critical shear section.

It is to be noted that in the British code, the critical section for shear is considered at 1.5 d from the face of the column.

CEB-FIP MC-90 model code [10]

The punching shear resistance based on British code is given by Equation (3).

$$F_{sd} = 0.12 \zeta (100 \rho f_{ck})^{1/3} u_1 d \tag{3}$$

Where; $\zeta = 1 + \sqrt{\frac{200}{d}}$

u₁ is the length of perimeter at 2d from the face of the column.

Euro code 2 [11]

The punching shear resistance based on Euro code 2 is given by Equation (4).

$$V_{Rd1} = \tau_{Rd} k (1.2 + 40 \rho_1) d \tag{4}$$

Where;

τ_{Rd} is shear strength equal (0.25f_{ctk}/γ_c)

k is factor equal (1.6 - d)

ρ₁ is ratio equal (ρ_x + ρ_y)/2 ≤ 0.015

d is effective depth of the slab equal (dx+dy)/2

Egyptian code [12]

The punching shear resistance based on Egyptian code is given by Equation (5).

$$q = \frac{Q \cdot \beta}{b_o \cdot d} \leq \sqrt{\frac{F_{cu}}{\gamma_c}} \tag{5}$$

Where;

Q is the design shearing force.

β is a factor depending on the location of the column.

d is effective depth of slab.

b_o is the critical perimeter length.

In this section, the experimental failure loads obtained in this set of experimental tests are compared with the predictions of different codes. The calculated punching shear values for all the slabs specimens are reported in Table IV. From the results presented in Table IV, it may be observed that CEB-FIP MC-90 model code, considering in the last one the real maximum aggregate size, provides predicted punching resistance values close to those obtained experimentally, with an average ratio for V_{exp}/V_{code} of 0.97 and 1.08, respectively.

Table- IV: Calculated punching shear capacity for slabs.

	Exp. P _u ,kN	ACI 318-95	BS 8110	CEB- FIP 97	EUR	ECP
S1-0	432	1.27	3.10	0.97	1.67	1.88
S2-20	431	1.33	3.20	1.00	1.87	1.98
S3-35	443	1.38	3.20	1.04	1.97	2.05
S5-60	439	1.36	3.30	1.03	1.95	2.03
S6-50	438	1.47	3.50	1.08	2.05	2.12
S7-70	400	1.45	3.30	1.04	2.08	2.16

IV. FINITE ELEMENT

The computer program ANSYS [13], was used to carry out the analyses. The punching behavior of two-way reinforced concrete slabs was modelling by the Solid 65, was used to model the concrete, link 8 was used to model the steel reinforcement and solid 45 was used to model steel plate. The symmetry boundary conditions were set first. The model being used is symmetric about two planes.

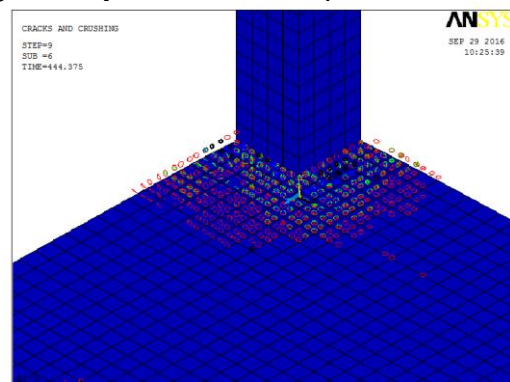




Fig. 7. Crack pattern and mode of failure S1-0.

A. Punching shear capacity and deflection

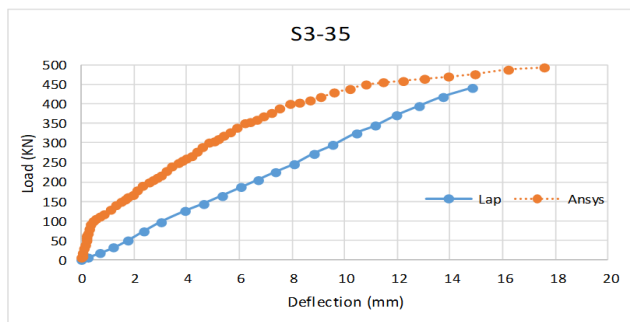


Fig. 8. Load deflection curve S3-35.

Table- V: Calculated punching shear capacity for slabs.

Slab ID	Experimental		Ansys model		Ansys/Exp	
	Load (kN)	Deflection (mm)	Load (kN)	Deflection (mm)	Load	Deflection
S1-00	432	17	444	12	1.02	0.73
S2-20	431	19	444	12	1.03	0.60
S3-35	443	15	494	18	1.11	1.20
S5-60	439	24	468	13	1.06	0.53
S6-50	438	17	484	14	1.10	0.84
S7-70	400	18	360	9	0.90	0.50

It's clear from Fig.7 that failure mode by ANSYS model was punching failure around column. Fig.8 and Table V show the load deflection curve of S3-35 and the predicted values computed using ANSYS model show better estimate of punching slabs load capacity, closer to the experimental failure loads and with a percentile of 1.06.

B. Crack pattern and mode of failure

The crack pattern of slab S2-20; the first crack under column at mid span, the cracks seem to be rounded than that of the control slab S1-0. Similar the crack pattern of slabs S3-35, S6-50 and S5-60 was the first crack at mid span under column. The first crack of slab S7-70 was at mid span under column at load 139 KN, and then cracks propagate till failure occurred between three major orthogonal cracks see Fig.9.

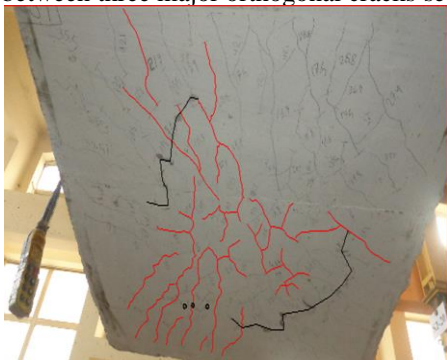


Fig. 9. Crack pattern and mode of failure S2-20.



Fig. 10. Crack pattern and mode of failure S3-35.



Fig. 11. Crack pattern and mode of failure S6-50.

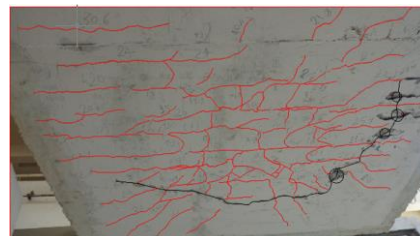


Fig. 12. Crack pattern and mode of failure S5-60.

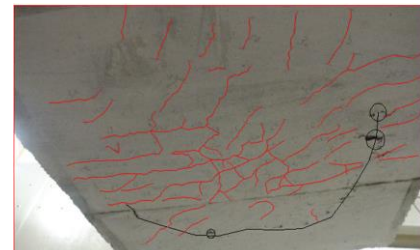


Fig. 13. Crack pattern and mode of failure S7-70.

V. CONCLUSION

1. It can be noticed that as the crushed ceramics percentage increases, the load increases until 35% ceramics percentage then the load decreases.
2. Recycled ceramics concrete aggregate prevented large cracks and enabled the slabs to maintain their shear punching capacity.
3. It was conclude that performance of recycled ceramics concrete was identical to that of the normal concrete.
4. Although the difference in the percentage of crushed ceramics and the failure load, the failure mode, and the crack pattern didn't change than the control specimen.
5. The results of specimen agree with the CEB-FIP MC-90 model code more than other codes.
6. The finite element model predicted the ultimate shear punching load capacity.
7. The finite element model predicted the mode of failure and crack pattern observed in the experiments accurately.



REFERENCES

1. Moore, D., Lennon, T., Wang, Y. 2007. "Designers' Guide to En 1991-1-2, 1992-1-2, 1993-1-2 and 1994-1-2: Handbook for the Fire Design of Steel, Composite and Concrete Structures to the Eurocodes", Thomas Telford Services Ltd.
2. Mehrafarid Ghoreishi, Ashutosh Bagchi and Mohamed A. Sultan "Estimating the Response of Flat Plate Concrete Slab Systems to Fire Exposure" structures in fire, of the 16-international conference, East Lansing, MI, USA, June 2-4 2010, PP. 286-293.
3. Amir Javed, Salman Siddique, Ram Prasad V S, "Investigation on ceramic waste and stone dust as aggregate replacement in concrete", International Journal of Engineering Technology, Management and Applied Sciences, March, Vol.3, pp.127-130, 2015.
4. Nuno Reis, Jorge de Brito, João R. Correia, Mário R.T. Arruda. Punching behavior of concrete slabs incorporating coarse recycled concrete aggregate Engineering Structures 100 (2015) 238–248.
5. Rao HS, Reddy VSK, Ghorpade VG. Influence of recycled coarse aggregate on punching behavior of recycled coarse aggregate concrete slabs. Int J Mod Eng Res 2012;2(4):2815–20.
6. ASTM C 39. Test method for compressive strength of cylindrical concrete specimens. Annual Book of ASTM Standards, 04.02, 1988:19-23.
7. DIN 50145 (1975) Testing of Metallic Materials; Tensile Test.
8. American Concrete Institute: ACI 318M-11. Building code requirements structural concrete and commentary; September 2011.
9. British code BS 8110 for design of concrete structures.
10. Fib model code for concrete structures 2010. Ernst & Sohn; October 2013. 434 pp.
11. European Committee for standardization. EN 1992-1-1 Eurocode 2: design of concrete structures – Part 1-1: general rules and rules for buildings; 2004.
12. Egyptian Committee for standardization. ECP 203-2018: design of concrete structures; 2018.
13. ANSYS theory manual.

AUTHORS PROFILE



Dr. Wael Ibrahim. Instructor of Concrete Structures and Steel Structures at the faculty of engineering, Helwan University. Well experienced in both steel and concrete structural design and construction supervision.

EDUCATION

PhD in Civil and Environmental Engineering, University of Aachen, RWTH, Germany September- 2011 M.Sc. of Structural Engineering Faculty of Engineering - Mataria, Helwan University, Cairo, Egypt July 2002 B.S. in Civil Engineering, grade very good with honor degree Faculty of Engineering - Mataria, Helwan University, Cairo, Egypt May 1996.

Dr. Amal Zamrawi. Instructor of Concrete Structures at the faculty of engineering, Helwan University. Well experienced in concrete structural design.

EDUCATION

PhD in Civil and Environmental Engineering, University of Helwan, Cairo, Egypt September- 2019 M.Sc. of Structural Engineering Faculty of Engineering - Mataria, Helwan University, Cairo, Egypt July 2013 B.S. in Civil Engineering, grade very good with honor degree Faculty of Engineering - Mataria, Helwan University, Cairo, Egypt May 2009.